Design of a Compact Low-loss Phase Shifter based on Optical Phase Change Material

Nikhil Dhingra, Junchao Song, *Student Member, IEEE*, Geetika J. Saxena, Enakshi K. Sharma, *Member, IEEE*, and B. M. A. Rahman, *Fellow, IEEE*

***Abstract*—We propose the design of a nonvolatile, low-loss optical phase shifter based on optical phase change material (O-PCM). The optical phase change material $Ge_2Sb_2Se_4Te_1$ (GSST), which exhibits low loss at telecommunication wavelength 1.55 μm as compared to other commonly used O-PCMs, is used in this work as the active material. Instead of direct interaction of the waveguide mode with the O-PCM, the design utilizes coupling between the primary SiN strip waveguide and a waveguide formed by O-PCM, in its amorphous state. The phase matching in the amorphous state inhibits the interaction of the waveguide mode with GSST in its highly lossy crystalline state resulting in low loss operation. Due to a high differential refractive index between the two states of GSST, the design requires a very small length of the phase shifter to accumulate the desired phase difference. The overall response of the Mach-Zehnder Interferometer (MZI) configuration using the designed phase shifter shows that the design can be used to obtain optical switching with a very small insertion loss and crosstalk over the entire C-band.**

***Index Terms*—Coupled mode analysis, Optical Switches, Phase change materials.**

I. Introduction

Phase shift for optical switching in silicon photonic devices is mainly achieved by free carrier injection [1-3] and thermo-optic effects [4]. These effects give rise to a small change in the refractive index, which results in large device length to obtain the required phase change. The alternative is to use the resonant structures to obtain devices with a small footprint, however, at the expense of low bandwidth and high sensitivity [5,6]. The compact hybrid plasmonic-photonic switches based on 3-waveguide directional couplers have also been reported, but the associated insertion loss is high [7,8]. In recent years, optical phase change materials (O-PCMs) have emerged for various photonic applications [9-14]. The O-PCM can be transitioned between the amorphous and crystalline phase with very different optical and electrical properties. The high differential refractive index between the two states can be utilized to obtain the desired phase shift, for modulation or switching, in a small length. Another important property of O-PCM is the non-volatile nature, i.e., power is required only during the transition events unlike other materials which require continuous power in at least one state. Depending on the technique used to change the state of the phase change material, the devices can be classified as thermo-optic, electro-optic or all optical.

The main challenge with the use of O-PCMs, for example, $Ge_2Sb_2Te_5$ (GST), is the high loss associated with crystalline state in the telecommunication band. This limits their use to devices which exploit the differential loss between the two states such as optical modulators [15,16]. Recently, Zhang *et al.* [17] reported a new optical phase change material $Ge_2Sb_2Se_4Te_1$ (GSST), which exhibits low loss in comparison to other commonly used PCMs. However, the loss in the crystalline state of GSST is still high and hence achieving low-loss switching using traditional Mach-Zehnder interferometer (MZI) based design was ruled out [18]. Zhang *et al.* [18] recently proposed the use of a non-perturbative design for switching based on O-PCMs using a three-waveguide directional coupler (3-wg DC), which promises low insertion loss and crosstalk.

In this letter, we propose the use of a GSST loaded SiN strip waveguide with a SiO_2 buffer layer to realize a compact phase shifter with low insertion loss for use in a traditional MZI configuration for low-loss switching. The proposed design allows a strong interaction between the waveguide mode and the GSST layer in its low loss amorphous state and hence requires a small volume of PCM, which in turns requires lower power to change the phase of PCM.

II. Design Criteria And Modal Analysis

The complex refractive index of GSST, at $\lambda = 1.55$ μm, are $5.074 - j0.425$ and $3.413 - j0.00018$ for crystalline and amorphous state, respectively [18]. In most of the earlier designs [18-21] based on silicon or silicon nitride, the O-PCM is used as an overlay directly on the primary waveguide as shown in Fig. 1(a). In such a configuration, the fundamental mode of the loaded waveguide interacts strongly with the O-PCM layer in its crystalline phase, due to its high refractive

This work was supported in part by University Grant Commission, India, in part by Erasmus Mundus INTACT program and in part by University of Delhi, India.

N. Dhingra, and E. K. Sharma are with the Department of Electronic Science, University of Delhi South Campus, New Delhi – 110021, India (e-mail: ndhingra@south.du.ac.in; enakshi@south.du.ac.in).

G. J. Saxena is with the Department of Electronics, Maharaja Agrasen College, University of Delhi, New Delhi – 110096 (e-mail: gsaxena@mac.du.ac.in).

J. Song, and B. M. A. Rahman are with Department of Electrical and Electronic Engineering, City, University of London, London EC1V OHB, U.K. (e-mail: junchao.song@city.ac.uk; B.M.A.Rahman@city.ac.uk).

index. As the imaginary part of refractive index is also large in the crystalline phase, this results in a very high loss. Hence, a low loss design needs to be such that there is strong interaction of the mode of the primary waveguide with the GSST overlay in its low loss amorphous state but is minimal for the crystalline state. To achieve this, we have considered a configuration based on SiN strip waveguide with a GSST overlay and introduced a SiO_2 buffer layer of thickness s between the primary waveguide and GSST layer as shown in Fig. 1(b). Such a structure behaves like a coupled structure formed by $SiO_2 - SiN - SiO_2$ strip waveguide (wg_1) and waveguide formed by $SiO_2 - GSST - SiO_2$ (wg_2). The width and height of the SiN strip are taken as 600 nm and 400 nm, respectively. For a given value of buffer layer thickness (s), the height (h_{GSST}) of the GSST layer can be adjusted such that the fundamental mode of wg_1 and wg_2 are phase matched, in amorphous state, to maximize the interaction with the GSST layer. For these parameters, the modes of the wg_1 and wg_2 will be phase mismatched in the crystalline state, due to a high difference in the refractive index of GSST in the two states.

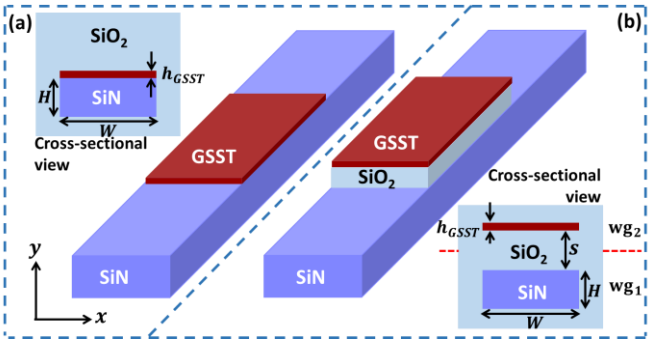

Fig. 1. 3D and cross-sectional view of the phase shifter (a) SiN waveguide with a GSST overlay (b) proposed design with SiO_2 buffer layer between GSST layer and SiN waveguide

The dominant H_y field of the quasi TE modes for the SiN waveguide with a GSST overlay of thickness $h_{GSST} = 58$ nm [Fig. 1(a)] are shown in Fig. 2(a) for both states of GSST. In Fig. 2(b), we have shown the modal profiles of the even and odd supermodes of the proposed design [Fig. 1(b)] of phase shifter for $s = 600$ nm and $h_{GSST} = 58$ nm for phase matching. The modes of the structures are obtained using the Finite Element Method (FEM) in Photon Design (version 6.1.2). As mentioned previously, for the GSST loaded SiN waveguide, the modal profile in Fig. 2(a) shows the strong interaction between the waveguide mode and GSST layer in crystalline state. For the proposed design of the phase shifter, it can be seen from Fig. 2(b) that the modal fields of both even and odd supermodes interacts well with the GSST layer, in amorphous state, due to phase matching as expected. On the other hand, in the crystalline state of GSST, the odd supermode is mostly confined to SiN waveguide and even supermode to GSST waveguide. If the phase shifter section is excited from an input SiN waveguide, both the even and odd supermodes are almost equally excited in the amorphous state of GSST. For crystalline state of GSST, only odd supermode gets excited due to negligible overlap of SiN waveguide modal field with the even supermode.

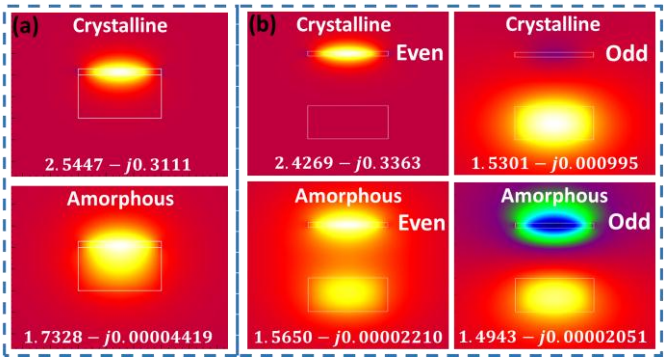

Fig. 2. (a) Modal profiles (H_y) of the quasi-TE modes of GSST loaded SiN waveguide [Fig. 1(a)] in the crystalline and amorphous states; (b) Modal profiles of the even and odd supermodes of the proposed structure [Fig. 1(b)] in the crystalline and amorphous states

Since wg_1 and wg_2 are phase matched in amorphous state around the chosen parameters, power couples out from wg_1 to wg_2. To ensure that power couples back to wg_1, the length of the phase shifter L_p has to be chosen to be twice the coupling length L_c^{am}, given by $L_c^{am} = \lambda/[2(n_e^{am} - n_o^{am})]$. In addition, we require a phase difference of π radians between the odd supermode in crystalline state with both even and odd supermode in amorphous state. This requires the following conditions to be satisfied:

$$\frac{2\pi}{\lambda_o}(n_e^{am} - n_o^{cr})L_p = \frac{2\pi}{\lambda_o}(n_o^{cr} - n_o^{am})L_p = \pi \qquad (1)$$

where, n_o^{cr} represents the effective index of the odd supermode in crystalline state and n_e^{am} and n_o^{am} are the effective indices of the even and odd supermodes in the amorphous states respectively. To find the parameters which satisfy the above conditions, we plotted the variation in the effective index of the supermodes as a function of h_{GSST} for various values of s in Fig. 3.

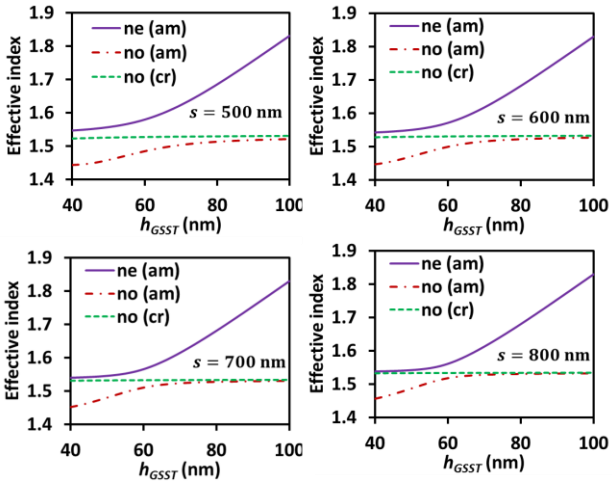

Fig. 3. Variation in the effective indices of supermodes supported by the phase shifter as a function of h_{GSST} for different values of buffer thickness s

It can be seen that the value of h_{GSST} for a given spacing s which satisfies Eq. (1) is almost same as the one for phase matching between the fundamental mode of wg_1 and wg_2 since $n_o^{cr} \approx n_{eff}^{SiN}$ and for the phase matched coupled waveguides $(n_e^{am} - n_{eff}^{SiN}) = (n_{eff}^{SiN} - n_o^{am})$. The value of h_{GSST}, which satisfies Eq. (1), is obtained as 58 nm. The

length of the phase shifter is calculated using the effective indices of the supermodes for different values of s using,

$$L_p = \frac{\lambda}{2(n_e^{am} - n_o^{cr})} = \frac{\lambda}{(n_e^{am} - n_o^{am})} = 2L_c^{am} \quad (2)$$

The required value of L_p and the imaginary part [imag(n_o^{cr})] of the effective index of the odd supermode in crystalline state are plotted in Fig. 4(a) as a function of s. It can be seen that L_p increases with increase in the value of s while imag(n_o^{cr}) decreases with an increase in s. The decrease in the value of imag(n_o^{cr}) is the dominant factor and hence the total attenuation, which is proportional to the product $L_p \times$ imag(n_o^{cr}), decreases with an increase in s. This is evident from Fig. 4(b), where we have plotted the power transmission coefficient $|S_{21}|^2$ for the phase shifter as a function of s using Eigen Mode Expansion (EEM) in Photon Design (version 6.1.2). The percentage difference between the required phase accumulation difference of π and the values obtained for our design through EEM simulations is also shown in Fig. 4(b) to be less than 3% for the entire range of spacing. Choosing a higher value of spacing results in low loss in both crystalline and amorphous states, however, requires a large length of phase shifter which in turn requires more power to change the state of GSST.

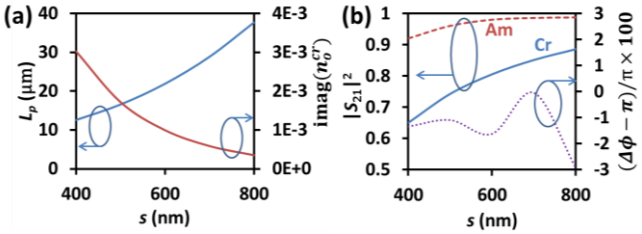

Fig. 4 (a) Variation in the length of phase shifter and imaginary part of the effective index of odd supermode in crystalline state as a function of s, (b) The $|S_{21}|^2$ parameter for phase shifter in crystalline and amorphous state, and percentage difference between the obtained and required phase accumulation difference value as a function of s

For $s = 600$ nm with corresponding $h_{GSST} = 58$ nm, the propagation through the phase shifter is shown in Fig. 5 for both states of GSST. As the choice of the length of phase shifter also makes it equal to the twice of the coupling length in the amorphous phase, the power returns to the primary waveguide at the end of the phase shifter with a small loss.

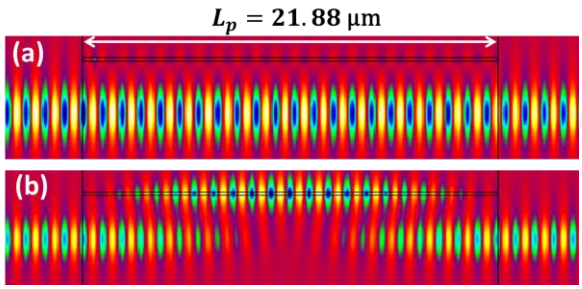

Fig. 5. The propagating TE mode field (H_y) through the phase shifter with GSST in (a) crystalline state (b) amorphous state

We also look at the response of the MZI switch with the designed phase shifter in one of its arms. The schematic of a typical MZI based switch, where DC_1 and DC_2 are ideal 3-dB directional couplers, is shown in Fig. 6. The output as a function of input can be obtained by the transfer matrix method as

$$\begin{bmatrix} E_1^{out} \\ E_2^{out} \end{bmatrix} = [A] \begin{bmatrix} S_{21} & 0 \\ 0 & e^{-j\phi_r} \end{bmatrix} [C] \begin{bmatrix} E_1^{in} \\ E_2^{in} \end{bmatrix} \quad (3)$$

where, E_i^{in} and E_i^{out} are the electric field at the i_{th} input and output ports, respectively; ϕ_r represents the phase accumulated by the reference arm; [A] and [C] are given by,

$$[A] = [C] = \frac{1}{\sqrt{2}} \begin{bmatrix} 1 & -j \\ -j & 1 \end{bmatrix} \quad (4)$$

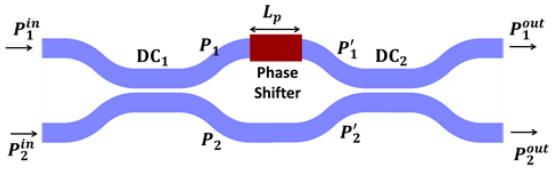

Fig. 6. Schematic of a MZI based 2x2 switch

The insertion loss (IL) and crosstalk (CT) obtained for both cross and bar states are shown in Fig. 7 as a function of L_p and volume of GSST, for corresponding spacing plotted in Fig. 4. The length of the reference arm is chosen such that it is phase matched with the phase shifter arm, in its amorphous state. It can be seen that the IL and CT are lower for designs with large value of phase shifter length; however, it will require higher volume of GSST and hence higher power to induce the phase change in GSST. For inducing the phase change in GSST through joule heating, a 30 nm ITO strip, with a free carrier concentration 1×10^{20} cm^{-3} and refractive index $1.816 - j0.025$, can be used as an overlay directly above the GSST strip. With the ITO strip, the optimized values of h_{GSST} and L_p, corresponding to $s = 600$ nm, were obtained as 54 nm and 21.96 μm, respectively.

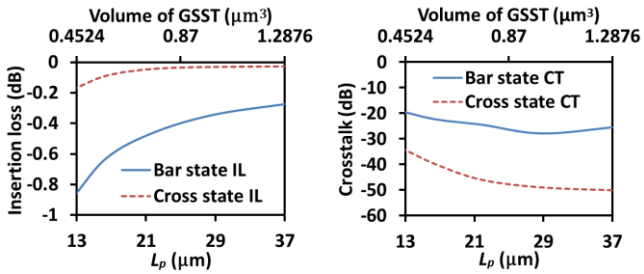

Fig. 7. Insertion loss and crosstalk as a function of the required length of the phase shifter and volume of GSST

In Fig. 8 we have shown the wavelength response for the proposed design ($s = 600$ nm) in terms of IL and CT. A significant effect of ITO loss is observed only in the cross state due to strong interaction with the GSST waveguide in the amorphous state. The value of IL is less than 0.6 dB and CT better than -20 dB over the entire C-band.

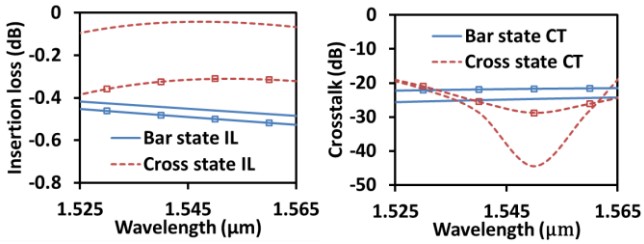

Fig. 8. IL and CT without ITO (without markers) and with ITO (with markers)

The maximum IL, CT and volume of GSST required for the proposed design of phase shifter, at $\lambda = 1.55$ μm, are summarized in the Table I along with the corresponding results for 3-wg DC [18] and traditional MZI [18]. The traditional MZI, with a GSST loaded SiN waveguide, exhibits a very high IL and CT; hence, it is not feasible for switching. On the other hand, the IL and CT for both 3-wg DC and proposed design are much better than the traditional MZI. However, the proposed design requires approximately half the volume of GSST in comparison to the 3-wg DC based design and hence will require lower power to induce phase change.

TABLE I
PERFORMANCE METRICS FOR DIFFERENT 2×2 SWITCH DESIGNS

	Traditional MZI	3-wg DC [18]	Proposed design
IL (dB)	$3.5^{[18]}$	0.32	0.5
CT (dB)	$-6.1^{[18]}$	-32	-24.5
GSST vol. (μm^3)	$0.04^{[calculated]}$	≈ 1.44	0.76

To study the fabrication tolerances, we calculated the IL and CT as a function of variation in H, s, W and h_{GSST}. For the cross state, the phase shifter (with GSST in amorphous state) acts as a directional coupler and hence the fabrication tolerances, shown in Fig. 9, are limited by the phase matching and dependence of coupling length on geometrical parameters. Bar state IL and CT do not show much variation as only one (odd) supermode gets excited in the crystalline state of GSST. Further, the fabrication tolerances can be improved by utilizing an adiabatic design of DC for the phase shifter [22].

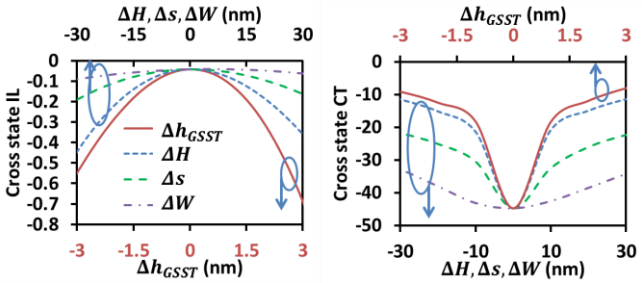

Fig. 9. IL and CT for the cross state as a function of variation in different parameters due to possible fabrication inaccuracies

III. CONCLUSION

Instead of simple interaction of the fundamental mode of a silicon or silicon nitride waveguide with GSST, we designed the phase shifter in such a way that it acts like a coupled structure. As the design utilizes the high overlap of waveguide mode with GSST layer in its low-loss amorphous state through phase matching and negligible overlap in lossy crystalline state, the design offers compact and low-loss switching across the entire C-band.

REFERENCES

[1] M. Nedeljkovic, R. A. Soref, and G. Z. Mashanovich, "Free-carrier electrorefraction and electroabsorption modulation predictions for silicon over the 1-14 μm infrared wavelength range," *IEEE Photonics J.*, vol. 3, no. 6, pp. 1171-1180, Dec. 2011.

[2] L. Lu, S. Zhao, L. Zhou, D. Li, Z. Li, M. Wang, X. Li, J. Chen, "16×16 non-blocking silicon optical switch based on electro-optic Mach-Zehnder interferometers," *Opt. Express*, vol. 24, pp. 9295-9307, 2016.

[3] L. Qiao, W. Tang, and T. Chu, "32×32 silicon electro-optic switch with built-in monitors and balanced-status units," *Sci. Rep.*, vol. 7, pp. 1-7, 2017.

[4] S. Chen, Y. Shi, S. He, and D. Dai, "Low-loss and broadband 2x2 silicon thermo-optic Mach-Zehnder switch with bent directional couplers," *Opt. Lett.*, vol. 41, pp. 836-839, 2016.

[5] H. Zhou, C. Qiu, X. Jiang, Q. Zhu, Y. He, Y. Zhang, Y. Su, and R. Soref, "Compact, submilliwatt, 2×2 silicon thermo-optic switch based on photonic crystal nanobeam cavities," *Photon. R.* vol. 5, no. 2, pp. 108-112, Apr. 2017.

[6] R. A. Soref, F. De Leonardis, and V. M. N. Passaro, "Mach-Zehnder crossbar switching and tunable filtering using N-coupled waveguide Bragg resonators," *Opt. Express*, vol. 26, no. 12, pp. 14959-14971, 2018.

[7] C. Ye, K. Liu, R. A. Soref, and V. J. Sorger, "A compact plasmonic MOS-based 2x2 electro-optical switch," *Nanophotonics*, vol. 4, no. 1, pp. 261-268, 2015.

[8] S. Sun, V. K. Narayana, I. Sarpkaya, J. Crandall, R. A. Soref, H. Dalir, T. Ei-Ghazawi, and V. J. Sorger, "Hybrid photonic-plasmonic non-blocking broadband 5x5 router for optical networks," *IEEE Photonics J.*, vol. 10, no. 2, pp. 1-12, Apr. 2018.

[9] M. Wuttig, H. Bhaskaran and T. Taubner, "Phase-change materials for non-volatile photonic applications," *Nat. Photonics*, vol. 11, pp. 465-476, Aug. 2017.

[10] K. J. Miller, R. F. Haglund JR, and S. M. Weiss, "Optical phase change materials in integrated silicon photonic devices: review," *Opt. Mater. Express*, vol. 8, no. 8, pp. 2415-2429, 2018.

[11] C. Rios, M. Stegmaier, Z. Cheng, N. Youngblood, C. D. Wright, W. H. P. Pernice and H. Bhaskaran, "Controlled switching of phase-change materials by evanescent-field coupling in integrated photonics," *Opt. Mater. Express*, vol. 8, no. 9, pp. 2455-2470, Sep. 2018.

[12] W. Dong, H. Liu, J. K. Behera, L. Lu, R. J. H. Ng, K. V. Sreekanth, X. Zhou, J. K. W. Yang, and R. E. Simpson, "Wide band gap phase change material tuned visible photonics," arXiv:1808.06459, 2018.

[13] J. Li *et al.*, "Extreme broadband transparent optical phase change materials for high-performance nonvolatile photonics," arXiv:1811.00526, 2018.

[14] J. Zheng, A. Khanolkar, P. Xu, S. Colburn, S. Deshmukh, J. Myers, J. Frantz, E. Pop, J. Hendrickson, J. Doylend, N. Boechler, and A. Majumdar, "GST-on-silicon hybrid nonphotonic integrated circuits: a non-volatile quasi-continuously reprogrammable platform," *Opt. Mater. Express*, vol. 8, no. 6, pp. 1551-1561, 2018.

[15] Z. Yu, J. Zheng, P. Xu, W. Zhang and Y. Wu, "Ultracompact electro-optical modulator-based $Ge_2Sb_2Te_5$ on Silicon," *IEEE Photon. Technol. Lett.*, vol. 30, no. 3, pp. 250-253, 1 Feb. 2018.

[16] B. Gholipour, J. Zhang, K. F. MacDonald, D. W. Hewak, and N. I. Zheludev, "An all-optical, non-volatile, bidirectional, phase-change meta-switch," *Adv. Mater.*, vol. 25, pp. 3050-3054, Apr. 2013.

[17] Y. Zhang, J. Li, J. B. Chou, Z. Fang, A. Yadav, H. Lin, Q. Du, J. Michon, Z. Han, Y. Huang, H. Zhang, T. Gu, V. Liberman, K. Richardson, J. Hu, "Broadband transparent optical phase change materials," in *Proc. Conf. Lasers Electro-Opt.*, San Jose, CA, USA, 2017, Paper JTh5C.4.

[18] Q. Zhang, Y. Zhang, J. Li, R. Soref, T. Gu, J. Hu, "Broadband nonvolatile photonic switching based on optical phase change materials: beyond the classical figure-of-merit," *Opt. Lett.*, vol. 43, no. 1, pp. 94-97, Jan. 2018.

[19] H. Zhang, L. Zhou, B. M. A. Rahman, X, Wu, L. Lu, Y. Xu, J. Song, Z. Hu, L. Xu, and J. Chen, "Ultracompact Si-GST hybrid waveguides for nonvolatile light wave manipulation," *IEEE Photonics J.*, vol. 10, no. 1, pp. 1-10, Feb. 2018.

[20] P. Xu, J. Zheng, J. K. Doylend, and A. Majumdar, "Low-loss and broadband nonvolatile phase-change directional coupler switches," *ACS Photonics*, vol. 6, pp. 553-557, Jan. 2019.

[21] F. De Leonardis, R. Soref, V. M. N. Passaro, Y. Zhang, and J. Hu, "Broadband electro-optical crossbar switches using low-loss $Ge_2Sb_2Se_4Te_1$ phase change material," *J. Lightw Technol.*, vol. 37, no. 13, pp. 3183-3191, July 2019.

[22] H. Yun, W. Shi, Y. Wang, L. Chrostowski, and N. A. F. Jaeger, "2 × 2 adiabatic 3-dB coupler on silicon-on-insulator rib waveguides," *Proc. SPIE*, vol. 8915, paper 89150V, May 2013.